Cancer Imaging (2013) **13(1),** 8–13
DOI: 10.1102/1470-7330.2013.0002

ORIGINAL ARTICLE

Interstitial laser-induced thermotherapy of the lung: evaluation of the influence of ablation continuity on ablation size in a swine model

Helmut Schoellnast[a,b], Sebastien Monette[c], Paula C. Ezell[d], Andrew Keene[e], Franz Quehenberger[f], Joseph P. Erinjeri[a], Stephen B. Solomon[a]

[a]Department of Radiology, Memorial Sloan-Kettering Cancer Center, 1275 York Avenue, New York, NY 10065, USA; [b]Department of Radiology, Medical University of Graz, Auenbruggerplatz 9, 8036 Graz, Austria; [c]Laboratory of Comparative Pathology, Memorial Sloan-Kettering Cancer Center, Weill Cornell Medical College, The Rockefeller University, 1275 York Avenue, New York, NY 10065, USA; [d]Research Animal Resource Center, Memorial Sloan-Kettering Cancer Center, Weill Cornell Medical College, 1275 York Avenue, New York, NY 10065, USA; [e]Visualase Inc., 8058 El Rio St. Houston, TX 7433, USA; [f]Institute for Medical Informatics, Statistics and Documentation, Medical University of Graz, Auenbruggerplatz 2, 8036 Graz, Austria

Corresponding address: Stephen B. Solomon, MD, Department of Radiology, Memorial Sloan-Kettering Cancer Center, 1275 York Avenue, H-118, New York, NY 10021, USA.
Email: solomons@mskcc.org

Date accepted for publication 1 November 2012

Abstract

The purpose of this study was to assess the relationship between size and the continuity of energy application in interstitial laser-induced thermotherapy. Percutaneous computed tomography-guided laser ablation (30 W, 600 nm diode) of the lung was performed in 7 Yorkshire pigs; a total of 42 ablation zones were created. Twenty ablations were performed using a continuous cycle of 2 min (protocol A) and 22 ablations were performed using 4 intermittent cycles with a duration of 1 min for each cycle interrupted by a 10-s stop between the cycles (protocol B). The lung was harvested immediately after euthanasia for gross pathology and histopathologic evaluation. Statistical analysis was performed using the Student *t* test and the Spearman correlation coefficient. Laser ablation resulted in complete necrosis of variable size of lung. The mean ablation zone dimensions (±SD) were 1.9 (±0.4) cm × 1.4 (±0.3) cm for protocol A and 2.2 (±0.5) cm × 1.4 (±0.4) cm for protocol B. The size of the necrosis is not significantly different when comparing a continuous 2-min ablation to a 4-cycle intermittent ablation for 1 min each cycle interrupted by a 10-s stop between the cycles ($P = 0.98$ and 0.53, respectively).

Keywords: *Laser ablation; laser-induced therapy; LITT; thermal ablation; lung.*

Introduction

Thermal ablation is a useful alternative treatment for patients with primary or secondary lung tumors. For thermal ablation of lung tumors, radiofrequency ablation (RFA) has been most commonly used. However, radiofrequency power delivery is limited by the intrinsically high impedance of normal lung tissue because of its high air content. Laser ablation (interstitial laser-induced thermotherapy (LITT), laser interstitial photocoagulation (LIP)) is a thermal ablation technique using optical fibers to deliver high-energy laser light to the target lesion, which absorbs the light energy as heat. The light is emitted to a distance of up to 12–15 mm through tissue, whereas the heat is conducted beyond this range creating a larger ablative zone[1,2].

In contrast to RFA, in which an impedance rise occurs at the transition zone between tumor and lung parenchyma resulting in a break of current flow, the laser functions with the irradiation of coherent monochromatic light, which is absorbed by the tissue and works independently of the impedance rise. A further advantage of LITT over RFA is that it can be combined with magnetic

resonance (MR) imaging, which allows real-time temperature monitoring using MR thermography. Modern systems utilize small high-power laser diode systems with actively cooled fibers to help keep tissue from charring during the procedure. Despite cooling the fibers, the duration and continuity of the energy application may influence the occurrence of charring of the tissue.

Groups that use LITT have reported that LITT produces a more predictable lesion shape than RFA because electrical conductivity does not affect heat deposition[3]. However, it remains unknown whether varying the laser application protocol can affect the size of the ablation zone in the lung. The aim of this experimental study was to assess whether a constant ablation size can be achieved in LITT of the lung and whether the continuity of ablation significantly influences the size of ablation.

Materials and methods

Animals

The study was approved by the Institutional Animal Care and Use Committee. Percutaneous computed tomography (CT)-guided laser ablation of the lung was performed in 7 Yorkshire pigs (weight 35–45 kg) from 2 suppliers (Archer Farms Inc., Darlington, MD; USA; Animal Biotech Industries, Inc., Danboro, PA, USA). Four to 8 ablations were performed per animal; a total of 42 ablation zones were created. Each procedure started with premedication using Telazol (4.4 mg/kg) intramuscularly and after intubation, general anesthesia was maintained via continuous inhalation of Isoflurane® (1.5–3%). Buprenorphine (0.01 mg/kg) was given via intramuscular injection before the start of each procedure. Euthanasia was performed immediately after the ablation session via intravenous injection of Euthasol (pentobarbital sodium 87 mg/kg and phenytoin sodium 11 mg/kg).

Laser ablation

Pigs were anesthetized and placed on the CT table (Lightspeed RTLS, GE Healthcare, Milwaukee, WI) in a prone position. Helical CT of the lung without contrast (collimation, 16×0.675 mm; section thickness 3 mm) was performed to plan the levels and the positions of the laser fiber entry. The skin overlying the entry positions of the probe was shaved and sterilized in the usual fashion using alcohol and betadine. A 30-W 600-nm diode laser with saline-cooled disposable laser fibers 1.65 mm in diameter (Visualase Inc., Houston, TX) was used in all experiments. Laser fibers were placed via a 14-G introducer needle, which was placed under CT guidance. Twenty ablations were performed in 4 pigs using a continuous cycle of 2 min at 30 W (protocol A) and 22 ablations were performed in 3 pigs using 4 intermittent cycles at 30 W for 1 min for each cycle interrupted by a 10-s stop between the cycles (protocol B). Correct fiber placement was ensured before and after each ablation with CT imaging. Ablations were performed randomly into different areas of the lung during normal ventilation avoiding proximity to vessels. Sequential CT scans covering the fiber and the ablation zone were performed after each ablation to measure the length and diameter of the ablation zones. The length and diameter were used to estimate the ablation volume by using an ellipsoid assumption, calculated as $\pi LD^2/6$, where L is the length and D is the diameter. Post-procedure pneumothoraces were treated with a 10-F pigtail catheter to ensure ventilated lung for the following ablations. Helical CT of the thorax (collimation, 16×0.675 mm; effective section thickness, 3 mm) was performed after the ablation sessions to finally evaluate the lung.

Gross pathology and histopathology

Immediately following euthanasia, a gross post-mortem examination of the chest was performed and the lungs were harvested. The entire lungs were axially sectioned at a thickness of 5 mm and the observed ablation zones were numbered and outlined on a graph to ensure adequate comparison with CT. The sections containing the ablation zones were incubated with 2% 2,3,5-triphenyltetrazolium chloride (TTC) at 37°C for 20 min, with rotation every 2 min to allow uniform tissue staining. The length and diameter of the ablation zones were recorded and the volumes were calculated for all ablation zones using the ellipsoid assumption described above. After measurement and photography, the sections were fixed in 10% neutral-buffered formalin for 24–48 h, after which they were routinely processed, embedded in paraffin, sectioned at 4-μm thickness, stained with hematoxylin and eosin (H&E), and examined by a pathologist (SM).

Statistical analysis

Statistical analysis was performed using an open-source statistical package (R, version 2.13.0; R Foundation for Statistical Computing, Vienna, Austria; www.r-project.org). P values < 0.05 were considered to indicate a significant difference. Differences between protocol A and B with regard to ablation zone length, diameter, and volume were tested by the Student t test on the mean value for each animal. Correlation between histologic and CT dimensions were tested using the Spearman correlation coefficient. Regression lines through zero, i.e. without intercept, were fitted through least squares.

Results

CT findings

Sequential CT after ablation revealed ablation zones as areas of consolidation and ground glass opacities with varying size (Fig. 1). Table 1 shows the mean value, standard deviation and the range of length, diameter, and volume for protocol A, protocol B, and both protocols.

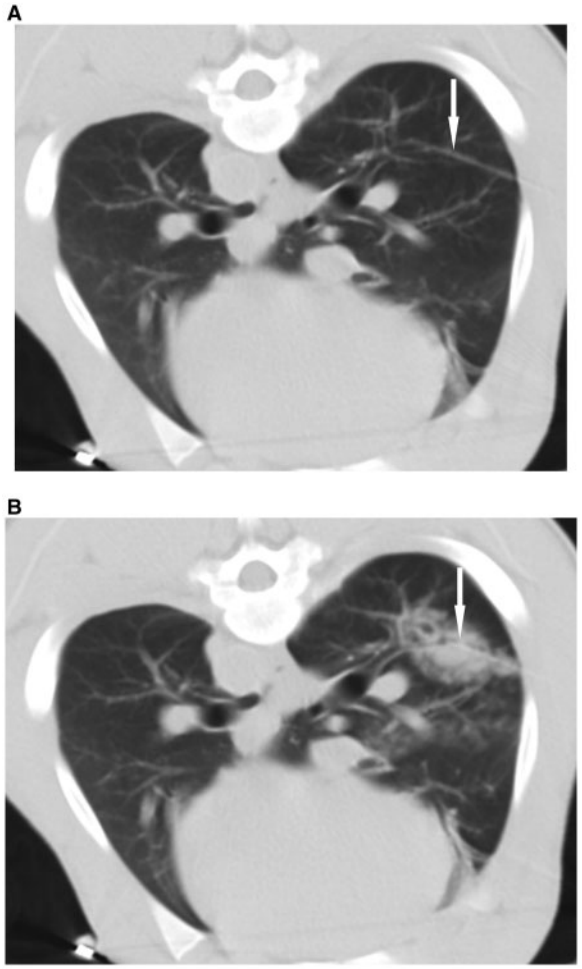

Figure 1 **(A) Non-enhanced CT before ablation demonstrating the laser fiber (arrow) to ensure adequate placement. (B) Non-enhanced CT immediately after ablation covering the laser fiber and the lesion to assess the lesion created, which is visualized as an area of consolidation and ground glass opacity (arrow).**

There was no statistically significant difference in diameter, length or volume of the ablation zones between protocol A and B (smallest *P* value 0.76).

Pneumothorax occurred in all pigs (1 side in 4 pigs and both sides in 3 pigs) and was treated in 4 pigs to ensure adequate lung aeration for further ablations.

Gross pathology

On gross examination, ablation zones were well-demarcated foci of brown discoloration (necrosis) of the pulmonary parenchyma, surrounded by a thin peripheral red rim (hyperemia). Thirty-eight ablation zones (90%) had a central focus of cavitation, 17 ablation zones in protocol A and 21 ablation zones in protocol B. The mean length and diameter of the cavitations (±SD) were 1.0 (±0.4) cm and 0.6 (±0.2) cm, respectively. Nineteen ablation zones (45%) extended to the pleura. Table 1 shows the mean value, standard deviation and the range of length, diameter, and volume for protocol A, protocol B, and both protocols. After staining with TTC solution, all ablation zones remained brown representing non-viable tissue necrosis, whereas the surrounding normal lung tissue was stained red representing viable tissue (Fig. 2). There was no statistically significant difference in diameter, length or volume of the ablation zones and of the central cavitations between protocol A and B (*P* values 0.98, 0.53, 0.65, and 0.30, 0.15, 0.25, respectively). There was no statistically significant effect of pleural contact of the ablation zone size with respect to diameter, length or volume (*P* values; 0.94, 0.69, 0.82).

Table 1 **Lesion size on CT and gross pathology[a] for protocol A, protocol B and both protocols**

		CT			Gross pathology		
		Mean	SD	Range	Mean	SD	Range
Protocol A ($n=20$)	Length (cm)	3.3	0.7	2.2–4.9	1.9	0.4	0.9–2.5
	Diameter (cm)	1.9	0.4	1.1–2.7	1.4	0.3	0.9–2.1
	Volume (cm^3)	6.9	3.7	1.5–16.0	2.0	1.1	0.4–3.1
Protocol B ($n=22$)	Length (cm)	3.4	0.5	2.3–4.2	2.2	0.5	0.9–3.1
	Diameter (cm)	2.0	0.4	1.2–2.8	1.4	0.4	0.6–2.0
	Volume (cm^3)	7.6	4.1	2.3–16.8	2.6	1.5	0.2–6.3
Protocol A + B ($n=42$)	Length (cm)	3.4	0.6	2.2–4,9	2.0	0.5	0.9–3.1
	Diameter(cm)	1.9	0.4	1.1–2.8	1.4	0.3	0.6–2.1
	Volume (cm^3)	7.2	3.9	1.5–16.8	2.3	1.3	0.2–6.3

[a]After staining with TTC and before fixation in formalin.

Correlation in ablation zone size between CT and gross pathology

The Spearman correlation coefficient between pathology and CT was 0.22 for length ($P=0.16$), 0.36 for diameter ($P=0.018$) and 0.44 for volume ($P=0.0036$). The correlations are shown in Fig. 3. There is a clear deviation of the slope of the regression line from 1 (45°).

Histopathology

The zone of necrosis was characterized by coagulative necrosis of all structures (alveoli, airways, blood vessels). Necrosis was characterized by cytoplasmic hypereosinophilia and nuclear pyknosis, although these cellular changes were often mild, due to the acute nature of the injury. The necrotic zone showed alveolar edema, which tended to be located at the periphery of this zone. An empty focus of cavitation was present in the center of the necrotic zone in 38 ablation zones (90%). There were thermal artifacts (nuclear streaming, basophilia of collagen) in the necrotic tissue, most prominently in the center. The periphery of the ablation zones showed a transition zone from necrotic to viable tissue. This zone showed mild to moderate hemorrhages and marked vascular hyperemia, and mild to moderate alveolar fibrin exudation. Figs. 4 and 5 demonstrate the 5 zones from the center to the periphery of the ablation zone: an empty area of cavitation, a zone of thermal artifacts, a zone of

Figure 2 **Staining with TTC solution shows the lesion with brown representing necrosis; the surrounding normal lung tissue is stained red representing viable tissue. Note the cavitation in the center of the lesion (dark brown, arrow).**

alveolar necrosis and edema, a zone of hyperemia of alveolar capillaries, and normal lung tissue.

Discussion

LITT and RFA are comparable in terms of thermal damage and side effects[4–7]. Most groups use RFA for thermal ablation of the lung, but LITT is preferred by some groups[3,7,8]; and it has been suggested that lung-specific conduction of laser light improves therapeutic success and tumor control compared with RFA[9]. Although the properties of lung tumors are different from the properties of normal lung tissue, normal lung tissue often surrounds tumors and may limit RF current flow, which may limit sufficient ablative margins or make the ablation zone less predictable. Rosenberg et al.[7] reported 1-, 3-, and 5-year survival rates of 81%, 44%, and 27% for patients who underwent LITT of pulmonary metastasis of different primary tumors. Similar overall survival has been reported for RFA in colorectal cancer lung metastases with an overall survival of 64–78% at 2 years[10]. The authors suggest that LITT has the potential to improve long-term survival among selected patients[7].

However, little literature is available on whether a constant ablation size can be achieved in LITT of the lung and whether the continuity of ablation significantly influences the size of ablation. In an ex vivo model, Ritz et al.[11] reported that the application of 28 W for 10 min using a 1064 nm Nd:YAG laser generated the largest ablation zones with a mean length of 3.9 ± 3.5 cm, a mean diameter of 2.5 ± 0.1 cm, and a mean volume of $12.5 \pm 1.3\,cm^3$. In an in vivo study, Fielding et al.[12] performed X-ray-guided LITT (2–3 W, 805 nm diode laser) of the lung in pigs and produced well-defined, localized ablation zones, typically 3.5×2 cm using up to 4 fibers.

In our in vivo study, the mean pathologic length of the ablation zone was 2.0 cm, the mean pathologic diameter

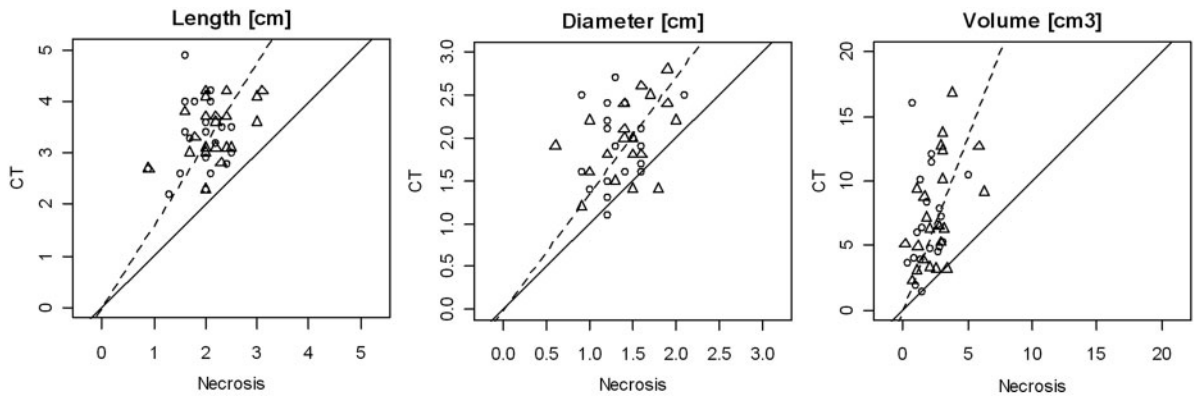

Figure 3 **Scatter plot of histologic necrosis versus CT lesion size. Measurements of protocol A are marked by squares; measurements of protocol B are marked by triangles. The solid line marks equal lesion sizes. The dotted line marks the best fit of a line through 0 and the observed measurements.**

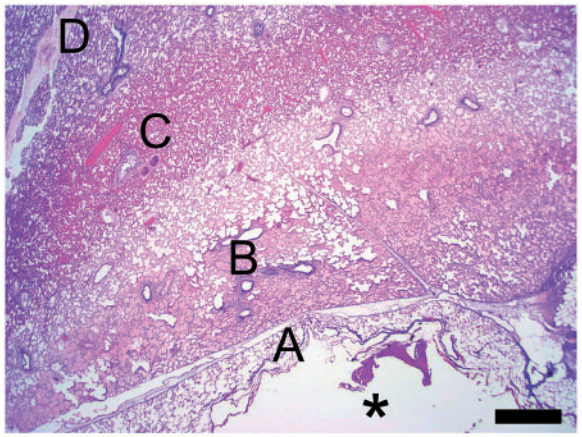

Figure 4 **Lesion, low magnification. From the center to the periphery of the lesion, 5 zones are observed: an empty area of cavitation (asterisk), a zone of thermal artifacts (A), a zone of alveolar necrosis and edema (B), a zone of hyperemia of alveolar capillaries (C), and normal lung tissue (D). H&E stain. Scale bar: 1 mm.**

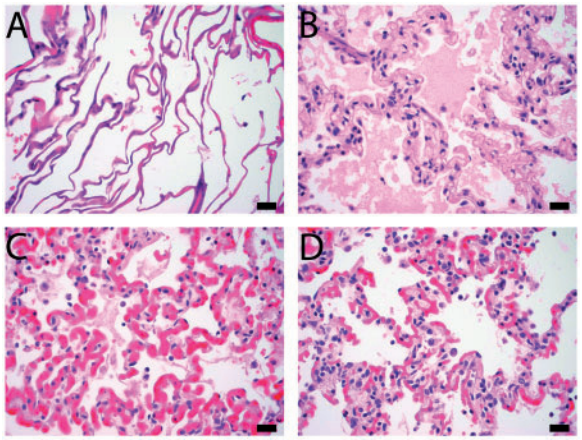

Figure 5 **Higher magnification of zones A, B, C, and D shown in Fig. 4. H&E stain. Scale bars: 20 μm.**

was 1.4 cm, and the mean pathologic volume was 2.3 cm^3 using 1 fiber. One can assume that ablation zone size is smaller in an in vivo model compared with an ex vivo model because ventilation and perfusion lead to cooling of the tissue. Ablation continuity using the 2 sampled parameters did not significantly influence the size of ablation. Mean pathologic ablation zone dimensions were 1.9 cm × 1.4 cm for a contiguous 2-min ablation (protocol A) and 2.2 cm × 1.4 cm for an intermittent ablation of 4 cycles for 1 min each cycle interrupted by a 10-s stop between the cycles to cool the fiber (protocol B). Both protocols led to similar variability in the size of the ablation zones. The range of the length of the ablation zones was 0.9–2.5 cm with the continuous protocol and 0.9–3.1 cm with the intermittent protocol; the range of the diameter was 0.9–2.1 cm with the continuous protocol and 0.6–2.0 cm with the intermittent protocol. Considering these ranges, the predictability of the ablation size in LITT seems not to be superior to that of RFA under uniform conditions in normal lung. Given the limited predictability and reproducibility, real-time monitoring, which is available for lung ablation using CT fluoroscopy, may be an accurate tool to ensure adequate ablation. One element of tissue variability is the location in the lung, which could provide differences in ventilation and perfusion as well as proximity to either insulative or conductive effects. In addition, proximity to larger vessels could provide more convective heat transfer away from the ablation (heat sink effect) thus limiting ablation zone size[13].

Ninety percent had a central focus of cavitation, which may be assumed as a result of charring. There was no statistically significant difference in diameter, length or volume of the central cavitations between protocol A and B.

The size of the lung ablation zones produced with LITT in our study was similar to the size of the lung ablation zones obtained with RFA in the literature. In a study by Brace et al.[10], RF energy was delivered through an internally cooled electrode with a 3-cm active length for 10 min. The authors reported a mean length of the ablation zones of 3.3 cm and a mean diameter of 2.1 cm. In a study by Oyama et al.[14], RFA was performed with a LeVeen needle with a maximum diameter of 3 cm and 4 retractable hooks. The authors reported a mean length of 2.1 cm, which is similar to the mean length achieved in our study with LITT. However, the time to ablate a certain volume of lung tissue was longer with RFA in the study by Brace et al.[10] than with LITT in our study. The ablation zone size measured on CT was larger than the ablation zone size in gross pathology. The mean length was 3.4 cm on CT and 2.0 cm in gross pathology; the mean diameter was 1.9 cm on CT and 1.4 cm in pathology. The difference between the size measured on CT and the size measured at pathology was likely due to the deflation of the lung at pathology compared with the inflated, in vivo images taken with CT. This is in accordance with a study on RFA of the lung that showed similar differences between CT size and size in pathology[10]. In this reported study[10], the mean length of the ablation zones was 4.3 cm on CT and 3.3 cm in pathology; the mean diameter was 3.1 cm on CT and 2.1 cm in pathology. Understandably then in our study, the Spearman correlation coefficient between CT and gross pathology was weak for the diameter; for the length there was no significant linear association between CT and gross pathology. Hemorrhage surrounding the ablation zones may also contribute to the variability in CT measurements as the laser fibers were placed via an introducer needle; and as a result, the border between the hemorrhage and the ablation zone was rarely clear. Therefore, CT measurements may have an error margin.

Several limitations of our study have to be considered. Although we attempted to place the laser fiber in the

center of the lung parenchyma, 19 ablation zones (45%) extended to the pleura. One can assume that this may have influenced the size of the ablation zones. However, statistical analysis did not show a significant effect of pleural contact of the ablation zones with respect to diameter, length or volume in our study. In addition, no statistically significant difference in progress between central and peripheral lesions has been reported in laser ablation of lung metastases[5]. The lack of randomization has to be considered as a further limitation, because the continuous and intermittent laser ablation protocols were applied in different pigs instead of applying both protocols in one pig. As this was a study under uniform conditions in normal lung, our results may not apply to treatment of lung tumors. Furthermore, the 10-s gap to reduce charring and the 1 min or 2 min of continuous power application were arbitrary values chosen for normal lung, and no conclusions may be drawn for lung tumors or for longer gaps and longer power application. In conclusion, LITT of normal lung parenchyma with a 30-W 600-nm diode laser with a saline-cooled disposable laser fiber led to complete necrosis of variable size. The size of the necrosis was independent of the use of a contiguous 2-min ablation or an intermittent 4-cycle ablation for 1 min each cycle interrupted by a 10-s stop between the cycles. Thermal equilibrium may limit ablation zone growth even with higher duration of energy application.

References

[1] Vogl TJ, Naguib NNN, Lehnert T, Nour-Eldin NA. Radiofrequency, microwave and laser ablation of pulmonary neoplasms: clinical studies and technical considerations–review article. Eur J Radiol 2011; 77: 346–357. PMid:19700254.

[2] Gough-Palmer AL, Gedroyc WM. Laser ablation of hepatocellular carcinoma–a review. World J Gastroenterol 2008; 14: 7170–7174. PMid:19084930.

[3] Hosten N, Stier A, Weigel C, et al. Laser-induced thermotherapy (LITT) of lung metastases: description of a miniaturized applicator, optimization, and initial treatment of patients. Rofo 2003; 175: 393–400. PMid:12635017.

[4] Simon CJ, Dupuy DE, DiPetrillo TA, et al. Pulmonary radiofrequency ablation: long-term safety and efficacy in 153 patients. Radiology 2007; 243: 268–275. PMid:17392258.

[5] Weigel C, Rosenberg C, Langner S, Frohlich CP, Hosten N. Laser ablation of lung metastases: results according to diameter and location. Eur Radiol 2006; 16: 1769–1778. PMid:16670870.

[6] Gillams AR. Complications of percutaneous therapy. Cancer Imaging 2005; 5: 110–113. PMid:16305947.

[7] Rosenberg C, Puls R, Hegenscheid K, et al. Laser ablation of metastatic lesions of the lung: long-term outcome. AJR Am J Roentgenol 2009; 192: 785–792. PMid:19234278.

[8] Vogl TJ, Straub R, Lehnert T, et al. Percutaneous thermoablation of pulmonary metastases. experience with the application of laser-induced thermotherapy (LITT) and radiofrequency ablation (RFA), and a literature review. Rofo 2004; 176: 1658–1666. PMid:15497085.

[9] Knappe V, Mols A. Laser therapy of the lung: biophysical background. Radiologe 2004; 44: 677–683. PMid:15221151.

[10] Brace CL, Hinshaw JL, Laeseke PF, Sampson LA, Lee Jr. FT. Pulmonary thermal ablation: comparison of radiofrequency and microwave devices by using gross pathologic and CT findings in a swine model. Radiology 2009; 251: 705–711. PMid:19336667.

[11] Ritz JP, Lehmann KS, Mols A, et al. Laser-induced thermotherapy for lung tissue–evaluation of two different internally cooled application systems for clinical use. Lasers Med Sci 2008; 23: 195–202. PMid:17599236.

[12] Fielding DI, Buonaccorsi G, Cowley G, et al. Interstitial laser photocoagulation and interstitial photodynamic therapy of normal lung parenchyma in the pig. Lasers Med Sci 2001; 16: 26–33. PMid:11486335.

[13] Steinke K, Haghighi KS, Wulf S, Morris DL. Effect of vessel diameter on the creation of ovine lung radiofrequency lesions in vivo: preliminary results. J Surg Res 2005; 124: 85–91. PMid:15734484.

[14] Oyama Y, Nakamura K, Matsuoka T, et al. Radiofrequency ablated lesion in the normal porcine lung: long-term follow-up with MRI and pathology. Cardiovasc Intervent Radiol 2005; 28: 346–353. PMid:15886942.